Manuscript File Click here to view linked References

Declining total carbon stocks in carbonate-containing agricultural soils over a 62-year recultivation chronosequence under humid conditions

Yi Zhao[1,2,3], Rüdiger Reichel[3], Michael Herbst[3], Yajie Sun[3,4], Nicolas Brüggemann[3], Ramona Mörchen[4], Gerd Welp[4], Fanqiao Meng[2]*, Roland Bol[3,5]

[1]*School of Chemistry and Environmental Engineering, Liaoning University of Technology, Jinzhou, Liaoning 121001, China*

[2]*Beijing Key Laboratory of Biodiversity and Organic Farming, College of Resources and Environmental Sciences, China Agricultural University, Beijing 100193, China*

[3]*Institute of Bio- and Geosciences, Agrosphere (IBG-3), Forschungszentrum Jülich GmbH, 52425 Jülich, Germany*

[4]*Institute of Crop Science and Resource Conservation (INRES), Soil Science and Soil Ecology, University of Bonn, 53115 Bonn, Germany.*

[5]*School of Natural Sciences, Environment Centre Wales, Bangor University, Bangor, LL57 2UW, U.K.*

* *Corresponding author. E-mail: mengfq@cau.edu.cn*

Abstract

Replanting of mining soils is necessary for utilizing soil resources and increasing cultivated land areas. However, limited information exists on the long-term temporal trends of carbon accrual in agricultural systems containing carbonate-rich soil material. We examined changes in soil organic carbon (SOC), soil inorganic carbon (SIC), and total carbon (TC) stocks in an agricultural soil containing carbonate over a 62-year recultivation chronosequence. The most critical differences in the SOC, SIC, and TC stocks were observed in the 0–30 cm soil layer. The results revealed that the SOC stock increased rapidly during the first 10–20 years, but only slowly thereafter. The SIC stock decreased over 62-year from approximately 40 Mg C ha^{-1} to 2 Mg C ha^{-1}. According to soil $\delta^{13}C_{TC}$ data, the SIC to TC ratio decreased from 83% (year 0) to 7% (year 62). Overall, the average sequestration rates were 0.30 Mg C ha^{-1} y^{-1} for SOC and −0.61 Mg C ha^{-1} y^{-1} for SIC over the 62 years after recultivation. Total carbon ultimately declined by approximately 19.5 Mg C ha^{-1} in recultivated carbonate soils. Topsoil SOC model (Rothamsted Carbon Model) outputs predicted an equilibrium value of 38.6 Mg C ha^{-1} after 197 years, which was less than the SIC stock lost in the first 70 years. Therefore, an overall TC increase in these carbonate-containing agricultural soils will only occur (i) during the initial rapid SOC sequestration accumulation phase (first 20 years of recultivation); and (ii) after the soils are fully decalcified (after ~62 years), but when SOC still slowly increases before SOC stocks reached full equilibrium (after ~197 years). However, compared with starting TC stocks, when we consider periods over a semicentennial and beyond, we will likely lose more TC than we gain in these recultivated agricultural soils if there are no additional TC sequestration measures.

Keywords: soil inorganic carbon; CO_2; restoration fields; RothC model; carbon sequestration; isotopic analysis

Introduction

Soils are the largest carbon (C) reservoir within Earth's terrestrial biosphere. The soil organic carbon (SOC) stock is approximately 1500–2400 Pg (Batjes, 1996; Stockmann et al., 2013), and that of soil inorganic carbon (SIC) is approximately 700–1750 Pg (1 Pg = 10^{15} g) (Batjes, 1996; Lal, 2007). Changes in soil C stocks can affect the global climate (Luo et al., 2010), and this has led to initiatives such as the '4 per 1000' (Minasny et al., 2017; Soussana et al., 2019). These initiatives have shown that soil carbon sequestration is a global soil climate-mitigation strategy and has positive effects on biodiversity, crop yields, and soil water retention (Rumpel et al., 2018; Soussana et al., 2019; Amelung et al., 2020).

Since the development of settled agriculture approximately 10–13 millennia ago, up to 25%–75% of the original SOC in the world's agricultural soils has been lost because of unsustainable intensive management practices (Lal, 2013). In Europe alone, 45% of soils have a low SOC content (Lehtinen et al., 2014). However, realising the actual global potential of SOC sequestration in agricultural systems remains challenging because it requires specific and varied options that are adapted to local soil conditions and management opportunities, and accounting for site-specific trade-offs (Amelung et al., 2020). Therefore, precise detailed information on what factors control and drive the agricultural soil C sink capacity and its turnover time in different soils is critical (Lal, 2013).

SIC also plays a crucial, but less reported, role in global C sequestration and CO_2 emissions (Lal, 2009; Chevallier et al., 2016). For example, Zamanian & Kuzyakov (2018) pointed out that, on a global scale, CO_2 emitted from liming of acidic soils was approximately 273×10^{12} g C y^{-1}. Additionally, emissions from carbonate-containing soil caused by nitrogen (N)

fertilization amounted to 7.5×10^{12} g C y^{-1}. Together, these numbers accounted for than 30% of total global CO_2 emissions from land use changes (Zamanian et al., 2018). Generally, in most agricultural systems under more humid conditions, SIC is low or absent. Therefore, research has so far mainly concentrated on SIC-related issues in semi-arid and arid areas of the world (Lardner et al., 2015). Such studies have revealed that agricultural management in semi-arid and arid regions often uses substandard and wasteful irrigation techniques to ensure maximum crop yields. However, during this process, Ca^{2+} and Mg^{2+} are partially leached down the profile, leading to deep soil pedogenic carbonate (PIC) formation (Bughio et al., 2017). Therefore, it is important to analyze changes in SIC in both topsoil and subsoil, not only for constraining CO_2 emission budgets, but also for overall assessment of the total soil C pool.

The recultivation of mining soil is necessary for re-utilization of soil resources. However, recultivated soils can vary greatly from original (pre-mining) soils. They may have lower nutrient status (Vindušková and Frouz, 2013), changes in the microbial biomass and microbiome (An et al., 2009; Li et al., 2015; Schmid et al., 2020) or mesofauna (Reichel et al., 2017), or a degraded soil structure (Lewis et al., 2010). These changes in soil quality result from mixing of the soil with other mining materials during and after the mining process (Schwenke et al., 2000).

The post-mining mineral soil may contain less SOC or have a different bulk density; therefore, the original SOC stock could also change. The SOC stock of recultivated post-mining soil is affected by factors such as the SOC input, inherent pedological characteristics, and the actual state of soil development (Rumpel et al., 2020). The new ‘steady-state’ SOC stock for a particular soil type is the result of the action of multiple soil processes and climatic conditions,

which are mediated by the specific management measures applied (Costantini et al., 2020; Rumpel et al., 2020). This process usually takes decades, which means that once a region's soil or its management measures are in a state of change, long-term observations are needed to comprehensively understand the SOC stock potential of each individual soil–climate combination (Lal, 2008; Costantini et al., 2020). It may also take a long time for recultivated soils to reach a new equilibrium condition, because the newly implemented management measures and soil characteristics may be extremely different from the original characteristics. Therefore, it is necessary to use models, such as the Rothamsted Carbon Model (RothC), to help estimate potential SOC changes and SOC stocks over semi- to multi-centennial timescales for re-cultivated soils.

When a retained pre-mining upper soil layer is mixed with mine-based materials containing inorganic carbon (e.g., carbonates), the newly reclaimed or post-mining soil has a higher inorganic carbon content than the original pre-mining soil (Zopes, 2017). Consequently, such soils are a potential source of CO_2 derived from inorganic carbon, and OC. This is an additional greenhouse gas emission issue that has not yet been adequately examined. Many recultivated post-mining soils are located in more humid parts of Europe, where SIC is not naturally present anymore in the soil (Clayton et al., 2021; Reichel et al., 2017). When SIC in the surface layer is dissolved over time, it leaches down the profile in the form of CO_3^{2-}, HCO_3^-, Ca^{2+}, and Mg^{2+}, and forms PIC in deeper layers. This SIC is then not truly lost from the overall soil total carbon (TC) pool, but just translocated. However, if the SIC is emitted as CO_2 or lost in a dissolved phase from the soil, then the SIC amount lost may exceed the amount of SOC sequestered at the initial stage of reclamation, because reclaimed soils usually have a higher SIC content

(Zopes, 2017). Then, SIC, and subsequently the TC content or stock, will decline (Bughio et al., 2015; Zamanian et al., 2018; Zamanian and Kuzyakov, 2018). However, whether the dissolved and leached SIC mainly forms PIC in the deep soil, or is irreversibly lost, still remains largely unexplored or unreported for humid regions of Europe and beyond.

Germany ranks first in the world for open-cast brown-coal production. As a result of mining activities, 313 villages in Germany have disappeared since 1924 and the use of approximately 180 km^2 of land has changed (Clean Energy Wire, 2018). The land recultivation rate after mining in Germany is among the highest in the world at 90% (Zheng et al., 2019). Consequently, there are many recultivated fields in Germany, and the time elapsed since restoration is longer than in most other countries (Roy et al., 2017). Some recultivation sequences have been initiated where SIC was freshly added when the new soils were reconstituted. This setting provides a unique opportunity to explore the longer-term SOC, SIC, and TC stock trends in restored agricultural fields to enable prediction of the time when new soil C will reach a steady state.

In the current study, we examined the temporal trends of SOC, SIC, TC, and total N (TN) stocks for the 0–30 and 0–90 cm layers of a 62-year agricultural recultivation chronosequence on sequentially restored farmland near an open-cast brown coal mine at Inden (Germany). We used ^{13}C isotope analysis to elucidate the farmland crop planting history and to assess the relative importance and fate of SIC and SOC in all soil C pools over time. The RothC model was used to simulate the SOC stock dynamics over a 500-year period after initiation of recultivation. We hypothesized that along the agricultural recultivation chronosequence i) SOC stocks would increase over time, but at decreasing rate; ii) SIC stocks would decline at faster rate than the SOC increase; and iii) TC stocks after 62 years would be lower than those measured

131 immediately after the start of the recultivation.

132

133 **2. Material and methods**

134 **2.1 Site description**

135 The sampling sites were located on restored farmland in an open-cast brown-coal mining area
136 in North Rhine-Westphalia, Germany (50°50′24″ to 50°53′30″ N, 06°14′20″ to 06°20′39.5″ E).
137 The climate in this area transitions from temperate oceanic to temperate continental. The annual
138 average temperature is 9.8 °C, the annual average rainfall is 829 mm per year, and the annual
139 average evapotranspiration is 601 mm per year. The average altitude is 124 m above sea level.
140 In this area, brown coal is extracted by the German energy company RWE after removing the
141 former agricultural soil and subjacent loess and sedimentary material. During the mining and
142 excavation process, the Luvisol of the former topsoil is mixed with the underlying parent
143 material. The new substrate is then used as a base for agricultural recultivation at the backside
144 of the mine.

145 Cultivation starts after soil substrate deposition. The recultivation process is divided into three
146 stages (Roy et al., 2017). In the first three years, the fields are planted with alfalfa (*Medicago*
147 *sativa* L.), fertilizer is applied at 200 kg ha^{-1} (mass ratio of $N:P_2O_5:K_2O$ = 15:15:15). Barley is
148 then planted for two years, and fertilizer is applied (437 kg ha^{-1} y^{-1}, containing 167 kg of N,
149 150 kg of P_2O_5, and 120 kg of K_2O). Finally, the fields are returned to farmers and managed
150 with common crop rotations, such as winter wheat/winter barley/sugar beet, in accordance with
151 standard German agricultural methods. The plough layer is 30 cm thick. The oldest farmland
152 sampled in this study was restored in 1956. Therefore, in 2018, when the 0–30 cm layer was

sampled, 62 years of land parcels were available for sampling along this agricultural recultivation chronosequence. Supplementary sampling of the 0–90 cm soil profile was undertaken in 2019, that is, in year 63 of the soil chronosequence.

2.2 Soil sampling

In ecology, it is difficult to find true replicates, especially for time series. True age replicates were unavailable in the study area. Therefore, we relied on within-field repetitions and the use of many sites to ensure that our age gradient was independent of field site effects. This method has been used in multiple previous studies in the same area (Reichel et al., 2017; Roy et al., 2017). For sampling, twelve fields with increasing time since recultivation (i.e., field age) and agricultural histories were selected (Fig. 1). The selected fields were restored in 1956, 1964, 1971, 1975, 1980, 1985, 1990, 1995, 2001, 2005, and 2011, which corresponded to recultivation times of 62, 56, 47, 43, 38, 33, 28, 23, 17, 13, and 7 years after their return to local farmers, respectively. The 2018 field was still fallow (i.e., the recultivation time was 0 years). Soil samples were collected in June 2018. We collected five samples from each field, which were taken at the vertices and center point of a square with a side length of 50 m. Soil samples were collected using a soil auger (diameter 3.0 cm) from 0–30 cm. The bulk density (BD) was determined by the ring cutter method during sampling. Plant roots were removed from the collected soil samples, and they were then air-dried, crushed, and passed through a 2.0-mm sieve to prepare them for determination of soil physical and chemical properties. Subsamples were milled and passed through a 0.15-mm sieve before SOC, SIC, labile organic carbon (LOC), residual oxidizable carbon (ROC), N, and isotopic analyses.

2.3 Soil analysis

Soil electrical conductivity (EC) was measured with a soil/distilled water ratio of 1:5, and soil pH was measured using 0.01 mol L^{-1} $CaCl_2$ solution (soil:$CaCl_2$ solution ratio of 1:5). Soil texture was measured by wet sieving (ISO 11277, 2020), which separated the soil samples into three particle-size fractions: sand (63–2000 μm), silt (2–63 μm), and clay (< 2 μm).

The SOC, SIC, LOC, and ROC contents were analyzed with a Soli TOC Cube (Elementar Analysensysteme, Hanau, Germany) at the University of Bonn, Germany. Each sample was analyzed in triplicate and a standard substance was analyzed after every 20 samples. The structure and measurement principles of the Soli TOC Cube are described by Mörchen et al. (2019), and details are given in the Supplementary Materials. Briefly, the Soli TOC cube distinguishes different forms of C by means of carrier gas switching and temperature programming. In a single program, LOC, ROC, SOC, and SIC can be measured separately. LOC is released at temperatures up to 400 °C, ROC is released between 400 °C and 600 °C in the case of dry combustion in a current of oxygen, and SIC is released at temperatures up to 900 °C. The SOC content was calculated using Eq. 1 and the TC content was calculated using Eq. 2.

$$\mathrm{SOC} = \mathrm{LOC} + \mathrm{ROC} \quad (1)$$

$$\mathrm{TC} = \mathrm{LOC} + \mathrm{ROC} + \mathrm{SIC} \quad (2)$$

The SOC and SIC stocks were calculated using Eqs. 3 and 4.

$$\mathrm{SOC_{stock}} = \mathrm{BD} \times \mathrm{SOC_{conc}} \times \mathrm{D} \quad (3)$$

$$\mathrm{SIC_{stock}} = \mathrm{BD} \times \mathrm{SIC_{conc}} \times \mathrm{D} \quad (4)$$

where D is the thickness of the soil layer, SOC_{conc} is the SOC content, SIC_{conc} is SIC content, and BD is soil bulk density. The TC stock was calculated as the sum of the SOC stock and SIC

stock. The TN contents were measured using a CN analyzer (Flash EA 2000, Thermo Fisher Scientific, Waltham, MA) at the Jülich Research Center (Jülich, Germany). TN was determined according to an established method (DIN, 2017).

Soil samples for analysis of the $\delta^{13}C$ values of SOC ($\delta^{13}C_{SOC}$) were ground and passed through a 0.15-mm sieve before soaking in 0.5 M HCl for 12 h to remove carbonates as described by Bughio et al. (2015). The soil was then dried in an oven at 60 °C. Samples were combusted at 1080 °C using a continuous flow system with a Flash 2000 (Thermo Fisher Scientific) elemental analyzer for carbon and a Euro EA 3000 (Eurovector) elemental analyzer for nitrogen. The elemental analyzer was directly attached to an isotope ratio mass spectrometer (Delta V Advantage, Thermo Fisher Scientific), and the measurements were conducted at the Jülich Research Center (Zhu et al., 2013). The $\delta^{13}C$ values of TC ($\delta^{13}C_{TC}$) were measured in a similar way as $\delta^{13}C_{SOC}$, but without the removal of the carbonates.

2.4 RothC model simulations of the SOC stock

RothC version 26.3 (Coleman and Jenkinson, 2005) was used to simulate the topsoil SOC stock with standard partitioning and turnover rates. The Downhill Simplex Algorithm (Nelder and Mead, 1965) was used for model inversion with RothC. The parameter settings in the RothC are described below.

TOC stocks were estimated according to the equivalent soil mass (Wendt and Hauser, 2013) from the organic carbon content and the reference Ap soil mass measured in 2018 in the plot that was refilled in 1956. The initial pools were assumed to be in equilibrium. First, the inert organic matter (IOM) pool was estimated from the SOC content at refill (8.8 Mg ha^{-1}) according to an established method (Falloon et al., 1998). The IOM pool was estimated as 0.58 Mg ha^{-1}.

Resistant plant material (RPM), microbial biomass (BIO) and humified organic matter (HUM) initial pools were estimated according to the pedotransfer functions (PTF) of Weihermüller et al. (2013). The initial decomposable plant material (DPM) was set to zero, because the overall DPM pool size was very small in relation to SOC (Table 1) and it equilibrated rapidly (Herbst et al., 2018).

Meteorological data for the air temperature, rainfall, and potential evapotranspiration were obtained from the German Weather service DWD for the period 1961–2018. Because refill occurred in 1956, which was defined as the model start, the 5-year gap between refill and the start of the metrological data was filled with monthly average meteorological data from the 1961–1971 period.

Model inversions were performed because reliable information about the cropping history and management was not available. However, the standard procedure for the first 5 years after refill was to plant legumes (without harvesting) before the plots were turned over to the farmers and subjected to standard agricultural practices. Therefore, we inversely estimated the C inputs for the first 5 years and used a different amount of yearly C input for the remaining 57 years. Yearly C inputs were assumed to consist of 50% organic amendments and 50% crop residues, which reflects typical agricultural practice in the study region (Herbst et al., 2018). Fifty percent of the crop residues were assumed to be incorporated in August each year, and the other 50% were assumed to be root exudates and evenly distributed between May and July.

According to the Summary for Policymakers of the Intergovernmental Panel on Climate Change (IPCC, 2018), global warming currently increases by 0.2 °C per decade, with a likely range of 0.1 °C–0.3 °C per decade. To predict the evolution of SOC for 24 future years, we

assumed a 0.2 °C increase in air temperature per decade. An increase in C inputs or changes in the water balance were not considered. We randomly selected 24 out of the 57 years in a meteorological time series and added the temperature trend of 0.2 °C per decade. This was repeated 100 times to account for inter-annual climate variability.

To run the model to equilibrium, we generated mean monthly meteorological data from the 1961–2018 time series. This average climatic year was repeated until the SOC stock of the recent year deviated from that of the previous year by less than by a factor of 0.005 of the recent year's SOC. The C inputs were assumed to be the same as those inversely estimated for the 1961–2018 period. The starting point for the equilibrium run was the C pools estimated after the first 5-year period of high C input. At that time, SOC stocks were 19.4 Mg ha^{-1}. The root mean square error between measured and estimated SOC stocks was 4.39 Mg ha^{-1}. There was some scatter in the measurements, which was probably related to heterogeneity of the parent material, and to variations in the crop rotation and management history at the specific plots. The inversely estimated C inputs for the first 5 years and the remaining 57 years were 5.98 Mg ha^{-1} y^{-1} and 3.50 Mg ha^{-1} y^{-1}, respectively.

2.5 Statistical analysis

Statistical analyses were performed using SAS (SAS Institute Inc., Cary, NC, USA). Data were tested for normality using the Shapiro–Wilk test and then one-way analysis of variance. Differences in soil pH, EC, and soil texture were determined by a *t*-test for least significant differences (LSD) at $P < 0.05$. The values are expressed as arithmetic means (n=5) with standard errors. Quadratic equations were used to estimate the relationships between ROC and the recultivation time. Exponential equations were used to estimate relationships between SOC

and TN content derived from the recultivation time. A linear model was used to estimate relationships between SIC and TC derived from the recultivation time.

3 Results

3.1 Soil physical and chemical properties

Analysis of changes in soil physical and chemical properties with recultivation time showed that soil pH gradually decreased with increasing recultivation time (Table 2). After 62 years of recultivation, soil pH had dropped significantly by 0.8 units. The sand and silt content did not change significantly with recultivation time. The clay content of soil that was recultivated for more than 33 years was significantly higher than that of soil recultivated for 0–28 years. Soil BD and EC showed no obvious trends (Table 2).

3.2 ROC, LOC, and SOC contents

The ROC content did not change in the first 28 years (~0.25 g C kg^{-1} soil). However, it significantly increased thereafter, with a peak value of 1.69 ± 0.20 g C kg^{-1} soil after 54 years and followed a quadratic curve (R^2=91.4%) (Fig. 2A). The LOC content rapidly increased in the first 13 years of recultivation, but the rate declined thereafter, with an exponential equation describing the trend best (R^2=60.1%) (Fig. 2B). The change in SOC content with recultivation time was very similar to the change in LOC, and was also best described by an exponential equation (R^2=59.6%) (Fig. 2C). The SOC content after 62 years of restoration was 7.12 ± 0.46 g C kg^{-1} soil, which corresponded to an increase of 4.77 g C kg^{-1} soil (203%) compared with the unrestored field (Fig. 2C). The ROC:SOC ratios were approximately 0.10, 0.05, and 0.18 for the unrestored field, the fields 7–28 years after restoration, and the fields 43–62 years after restoration, respectively. The highest proportion of the more stable ROC in the SOC pool

285 (18.2%) was found in the field 54 years after restoration (Fig. 3).

286 **3.3 SIC, TC, and TN contents**

287 The SIC content did not significantly change during the first 28 years (ca. 10–12 g C kg^{-1} soil;
288 Fig. 4A) but was decreased significantly after 33 years (by 7.1g C kg^{-1} soil) (Fig. 4A). From
289 33 to 62 years, the SIC content decreased linearly with increasing cultivation time (R^2=87.7%).
290 After 62 years, the SIC content was 0.53 ± 0.13 g C kg^{-1} soil, that is, 4.46 g C kg^{-1} soil or 89%
291 lower than after 33 years, and 10.91 g C kg^{-1} soil or 95% lower than that of the unrestored field
292 (year 0). The soil TC content clearly increased with the cultivation duration in the first 28 years
293 (Fig. 4B, R^2 =75.1%), but thereafter the TC content showed a significant linear decline from 33
294 to 62 years (R^2=71.0%). The field restored 28 years ago had the highest TC content (18.5 ±
295 0.88 g C kg^{-1} soil), which was 4.7 g C kg^{-1} soil (34%) higher than that in the unrestored field
296 (Fig. 4B). The TC content in the first 28 years increased on average by 0.17 g C kg^{-1} soil y^{-1}.
297 The 62-year-old field had the lowest TC content (7.65 ± 0.44 g C kg^{-1} soil), which was 40.3%
298 lower than that in the 33-year-old field (12.8 ± 1.51 g C kg^{-1} soil). Over the whole 62 years of
299 the recultivation chronosequence, the TC content decreased on average by 0.1 g C kg^{-1} soil y^{-1}
300 (Fig. 4B). The temporal change in soil TN content with recultivation time was similar to that of
301 SOC and could also be simulated by an exponential equation (Fig. 5, R^2=80.2%). The TN
302 content increased significantly during the initial 10 years, but the rate slowed considerably after
303 23 years. The TN content of the field 62 years after restoration was 0.84 ± 0.03 g N kg^{-1} soil,
304 which was an increase of 0.57 g N kg^{-1} soil (215 %) compared with the unrestored field (Fig.
305 5).

306 **3.4 $\delta^{13}C_{SOC}$, $\delta^{13}C_{TC}$, and soil carbon stock**

307 The $\delta^{13}C$ value of the soil organic carbon in the unrestored fields was −25.4‰ (year 0). The
308 $\delta^{13}C_{SOC}$ values of the recultivated fields after 7 to 62 years fluctuated between −28‰ and −26.5‰
309 and were independent of the duration of cultivation (Fig. 6A). The $\delta^{13}C_{TC}$ decreased
310 significantly with recultivation time (Fig. 6B). The $\delta^{13}C_{TC}$ of the unrestored field was −4.5‰,
311 and the $\delta^{13}C_{TC}$ of the 62-year-old field was −26.7‰ (Fig. 6B), which was similar to the value
312 of $\delta^{13}C_{SOC}$ (−27.4‰) in this field (Fig. 6A).
313 The SOC stock did increase with recultivation time (Table 3). After 7, 13, 23, 33, and 62 years,
314 the rates of SOC stock enhancement were 1.50, 1.35, 0.99, 0.69, and 0.30 Mg C ha^{-1} y^{-1},
315 respectively (Table 3). Therefore, the SOC stock increased fastest in the first 7 years of
316 recultivation. The SIC stock did not change significantly during the first 23 years of
317 recultivation (Table 3). The 28-year-old field had the largest SIC stock (47.2 ± 2.1 Mg C ha^{-1}).
318 By contrast, in the period from 33 to 62 years after the start of the recultivation, the SIC stock
319 decreased by 0.61 Mg C ha^{-1} y^{-1} (Table 3), and the lowest calculated value of 2.0 ± 0.5 Mg C
320 ha^{-1} was found after 62 years of recultivation. Compared with the unrestored field, SIC stocks
321 decreased by approximately 38 Mg ha^{-1} after 62 years.
322 The TC stock increased significantly, on average by 0.86 Mg C ha^{-1} y^{-1}, in the first 28 years of
323 recultivation (Table 3). After 28 years of recultivation, the estimated TC stock peaked at 72.3
324 ± 3.4 Mg C ha^{-1}. In the period from 33 to 62 years, the TC stock decreased significantly, with
325 an average decrease of 0.76 Mg C ha^{-1} y^{-1}. The TC stock of the 62-year-old field was 28.7 ±
326 1.7 C Mg ha^{-1}, which was 19.5 Mg ha^{-1} less than that of the unrestored field (Table 3).

327 **3.5 RothC-based SOC stock estimates**

328 Using RothC, we estimated that approximately 25.4 Mg ha^{-1} of C was sequestered over the 62-

329 year period, corresponding to an average sequestration rate of 0.41 Mg ha^{-1} y^{-1}. An equilibrium
330 state was reached after 197 years, which was associated with an equilibrium SOC stock of 38.6
331 Mg ha^{-1} (Fig. 7). It is noteworthy that a value of 36 Mg ha^{-1}, which is quite close to the
332 equilibrium stock of SOC, was reached after only 122 years. This occurred simply because of
333 the SOC increased exponentially and the rate of change near the maximum level was minimal.

334 **4 Discussion**

335 **4.1 Changes in SOC and other soil properties in the restored fields**

336 Studies have shown that SIC is the most important buffering system in carbonate-rich arable
337 soils to mitigate soil acidification caused by N fertilizer application (Huang et al., 2015;
338 Zamanian et al., 2018). Therefore, soil pH reflects the presence of SIC (as carbonate) to some
339 degree in soil throughout the chronosequence (Zamanian et al., 2018). Only when SIC
340 approached zero, a drop in soil pH of 0.5 units (i.e., from 6.9 to 6.4) was observed between the
341 54- and 62-year-old fields. Previous studies have suggested that there are almost no SIC stocks
342 in soils with a pH below 6.5 (Raza et al., 2020; Zamanian and Kuzyakov, 2018), which is
343 consistent with our study. The lack of clear temporal changes in BD and EC values reflect that
344 they are generally greatly affected by factors such as tillage, fertilization, irrigation, and planted
345 crops (Corwin and Lesch, 2003). Crop management in the study region is fairly unified, but
346 crops and their rotation patterns may differ between years. Therefore, in addition to the
347 recultivation duration, the number of crop rotations may contribute to interannual changes in
348 soil BD and EC.

349 The physico-chemical stabilization of SOC by clay particles is documented in the literature
350 (Bol et al., 2009; Six et al., 2002; Zhao et al., 2020). LOC is an unstable and easily oxidizable

C fraction that is generally derived from recently deposited and undecomposed plant residues and is mostly concentrated in the sand fraction (Amelung et al., 1999; Von Lützow et al., 2007). ROC is composed of microbially processed organic carbon compounds that form more stable organo-mineral associations, and is mostly concentrated in the clay fraction (Derrien et al., 2006; Grandy and Neff, 2008). In this study, the changes observed for ROC and clay with the reclamation time were not consistent. The reason for this may be heterogeneity in the texture of the reclaimed soil because of rapid soil development (weathering) in 62 years. Reclaimed soil can be affected by previous excavation processes. For example, if digging machines move in one direction (e.g., northward or eastward), slight artificial texture differences (e.g. clay content) can be introduced in the initial substrate used for recultivation. Consequently, the 'existing' soils and bedrock may differ slightly along a certain digging transect. Schwenke et al. (2000) found that SOC levels in mining areas could be restored after 33 years of reclamation with trees. In our study, we found that the SOC content after 28 years of recultivation was initially restored mainly in the form of LOC, whereas ROC increased significantly only after 38 years of recultivation. There were probably two reasons for this. First, the 'original' soil microbial community may have not been restored at the beginning of the recultivation (Kim et al., 2018; Stahl et al., 2003). The present microbial biomass or community structure (Reichel et al., 2017; Roy et al., 2017) only promoted a significant increase in ROC content after 38 years of recultivation. Secondly, the formation and turnover of ROC takes longer than that of LOC, and new ROC formation generally takes several decades (Meng et al., 2014; Six and Jastrow, 2002).

In this study, we simulated and predicted the SOC stock of the recultivated soil using the RothC

model. We also conducted a supplementary measurement of the SOC stock of deeper soil in June 2019. The results showed no significant differences in the SOC stock below a soil depth of 30 cm in the agricultural recultivation chronosequence (Fig. 1S). This means that analysis of SOC in the cultivated layer is important for the analysis and prediction of SOC changes in the region.

The $\delta^{13}C_{SOC}$ analysis showed that predominantly C_3 crop plants (e.g., wheat) were grown in the fields over the entire length of the chronosequence, with very limited evidence of the occasional presence of C_4 crops (e.g., maize), as only suggested by a slightly higher $\delta^{13}C_{SOC}$ value (−26.5‰**)** in the 47-year-old field. However, studies have revealed that for soil restoration purposes the recultivation time, rather than vegetation type, is the main factor affecting physical and chemical soil properties (Vindušková and Frouz, 2013; Kim et al., 2018). Therefore, although there are some differences in the crops grown in the restored fields, the changes in soil carbon are mainly affected by the reclamation time.

4.2 Changes in SIC in mining restoration fields

Hydrogen ions released in arable soil during the nitrification process after N fertilizer application may be the main factor causing SIC dissolution (Tamir et al., 2013; Yu et al., 2018). This is supported by the finding that nitrification inhibitors significantly reduce SIC dissolution in the plough layer (Li et al., 2017). The application of ammonium-based N fertilizer induces nitrification by ammonia-oxidizing bacteria and ammonia-oxidizing archaea (Firestone and Davidson, 1989). The number of ammonia-oxidizing archaea and ammonia-oxidizing bacteria directly affects the nitrification rate (Firestone and Davidson, 1989; Zhang et al., 2016). Therefore, we assumed that the change in SIC content with restoration time in our study was

related to the rate and duration of nitrification in the different fields of the recultivation chronosequence.

We did not find any significant change in SIC content between 0 and 28 years of recultivation. This was probably because of the low microbial activity, which was reflected in the low microbial biomass in the soil at the beginning of recultivation (Li et al., 2015; Reichel et al., 2017). This was associated with a low nitrification rate and low H^+ release, which led to only very limited dissolution of SIC. In our study, the SIC dissolution accelerated 33 years after the start of recultivation, and this probably occurred because the abundance and activity of nitrifiers increased significantly by then (Kim et al., 2018). In addition, the TN content increased rapidly during the first 10 years of recultivation, but the rate of increase slowed thereafter. This supported our assumption that the N loss associated with nitrification and denitrification was low at the beginning of the recultivation.

We also analyzed changes in SIC/TC and $\delta^{13}C_{TC}$ with reclamation time. While the $\delta^{13}C_{SOC}$ did not change significantly, the $\delta^{13}C_{TC}$ value gradually decreased with time. Therefore, according to the soil $\delta^{13}C_{TC}$ data, the ratio of SIC to TC decreased from 83% (year 0) to 7% (year 62) (Fig. 6, Fig. 2S, and Table 3). This was also evidence of continued nitrification throughout the 62 years of recultivation, which caused SIC dissolution. However, during the first 28 years, this process was too weak to significantly change the SIC content. In the future, the $\delta^{13}C_{TC}$ value could be used as a rough gross indicator of the relative proportion of SIC still present in wider soils in this area.

In this study, fields lost approximately 38 Mg ha^{-1} of SIC after 62 years of recultivation when compared with unrestored fields. Dissolved SIC can change into two forms: (1) CO_2, which is

417 emitted to the atmosphere; and (2) CO_3^{2-}, HCO_3^-, Ca^{2+}, and Mg^{2+}, which are leached to the
418 deep soil to form PIC and end up in groundwater or exported as soluble $Ca(HCO_3)_2$ or
419 $Mg(HCO_3)_2$ to surface water. PIC formation is higher at depth than in the cultivated layer
420 (Bughio et al., 2017). The results of additional experiments proved that there was no tendency
421 for SIC to accumulate in the deep soil in the same field and it was independent of the length of
422 recultivation (Fig. 3S).
423 Ca^{2+} and Mg^{2+} are required for SIC formation; therefore, their contents in soil can be used to
424 characterize SIC changes (Monger et al., 2015). We analyzed the Ca^{2+} and Mg^{2+} distributions
425 in the 0–90 cm soil profile. The results showed that in all three soil layers (0–30 cm, 30–60 cm,
426 and 60–90 cm), there were no significant differences in the Ca^{2+} and Mg^{2+} contents (Fig. 4S
427 and Fig. 5S). This suggested that Ca^{2+} and Mg^{2+} were not leached to deeper soil layers. Indeed,
428 most studies have shown that arable land, which is characterized by SIC accumulation in deeper
429 soil layers, is located mainly in arid and semi-arid areas, where SIC changes are greatly affected
430 by climate and irrigation (Lal, 2002). Fields in arid and semi-arid areas generally require
431 irrigation, and often high levels of Ca^{2+} and Mg^{2+} are present in irrigation water. The Ca^{2+} and
432 Mg^{2+} in irrigation water and the Ca^{2+} and Mg^{2+} produced by the SIC dissolution will be leached
433 with surplus irrigation water. Because of evapotranspiration, Ca^{2+} and Mg^{2+} will recombine
434 deeper in the soil profile with CO_2 to form PIC (Pan, 1999), and this will cause SIC
435 accumulation in the deeper soil (Entry et al., 2004; Sahrawat, 2003). The restored arable land
436 in our study is located in a humid region of Germany, where the annual rainfall is moderate and
437 evenly distributed. Irrigation measures are generally not required in this area, and there is
438 usually no secondary carbonate formation. Although it is possible for dissolved carbonate to

enter groundwater in the form of readily soluble calcium bicarbonate, there was no significant leaching of Ca^{2+} and Mg^{2+} in the 0–90 cm soil profile. Therefore, the dissolved SIC in the cultivated layer will be mainly emitted into the atmosphere as CO_2.

4.3 Potential for increasing the soil C pool in mining restoration fields

After analyzing the SOC and SIC stocks in the 62-year agricultural recultivation chronosequence and considering the simulated SOC stock changes in the restored fields, we divided the temporal soil C pool changes in this study into four phases. In the first phase (0–28 years), the SOC stock increased significantly, but there was no significant change in SIC. Therefore, the soil of the restored fields acted as a sink of CO_2 at this stage. In stage 2 (33–62 years), the SIC loss was significantly higher than the corresponding SOC increase, and the soil acted as a source of CO_2. In stage three (62–197 years), the SIC content almost completely disappeared within the cultivated layer, and the SOC continued to slowly increase. At this stage, cultivated fields once again acted as a sink of CO_2. Finally, in stage four (> 197 years), with no SIC present in the surface layer and SOC reaching equilibrium, the surface soil would be neither a sink nor source of CO_2. Overall, the largest TC (SOC + SIC) stock in the whole profile (0–90 cm) was found between 14 and 24 years after the start of recultivation (Fig. 6S), which indicated the process was in phase 1, as expected.

Recent research has suggested that CO_2 production from SIC caused by neutralization of N fertilization-induced acidity is globally relevant (Zamanian and Kuzyakov, 2018; Zamanian et al., 2018), and that SIC is an important CO_2 source with a critical impact on atmospheric composition (Chevallier et al., 2016; Tamir et al., 2013). Raza et al. (2020) showed that the application of N fertilizer in China reduced cropland SIC stocks (0–40 cm) by 7% (0.15 Pg C;

1.1 Mg C ha^{-1}) between 1980 and 2020. Zamanian et al. (2018) estimated that the global CO_2 efflux because of $CaCO_3$ dissolution following N fertilization was equivalent to 7.48×10^{12} g C y^{-1}. However, these previous studies considered SIC decomposition under natural distribution. They did not consider the soil CO_2 emissions from carbonate decomposition following restoration of (agricultural) fields post-mining. Our research highlights the large potential for SIC loss in the carbonate-containing soils following agricultural recultivation. The topsoil SIC loss (0.61 Mg C ha^{-1} y^{-1}) in this reclaimed arable land in Germany exceeds values measured for carbonate-containing agricultural soils in China; although, China is recognized as a country with high N fertilizer application rates (Potter et al., 2010) that are at least 2–3 times those in Germany (Löw et al., 2021). We speculate that there are two main reasons for this: (1) the SIC content in the arable soil in our study was twice that at the beginning of restoration in Chinese carbonate soils (~6–8 g C kg^{-1} soil) (Bughio et al., 2015; Bughio et al., 2017; Zhao et al., 2021); and (2) in the arid and semi-arid regions of China, part of the CO_2 produced after carbonate decomposition will be bound again in the form of PIC (Bughio et al., 2015; Entry et al., 2004; Sahrawat, 2003). However, in our study, almost all of the carbonate present in the surface soil of the reclaimed arable land was decomposed to CO_2 and released to the atmosphere. Therefore, post-mining SIC-derived CO_2 losses from restored carbonate-containing arable land should not be ignored at a global scale, especially for more humid regions.

The recultivation of fields post-mining resulted in large SIC losses over the 62 years, but should be set against other sustainability needs, for example, requirements to increase agricultural production areas to address higher global food requirements as the world population continues to grow (Spiertz and Ewert, 2009). Furthermore, although SIC did decline, SOC increased

overall. The natural water balance of the recultivation chronosequence in humid areas or insufficient input of external Ca^{2+} and Mg^{2+} may be the main reason that we could not detect any subsurface PIC formation in our study (Bughio et al., 2015; Pan, 1999). Our study highlights that it is essential to accurately quantify the effects of restoration of arable land on SOC and SIC sources and sink strengths for different regions of the world.

Conclusions

The most critical differences in the TC, SIC, and SOC stocks were observed in the upper 0–30 cm of soil for these recultivated agricultural soils. Here, the SIC to TC ratio gradually decreased from 83% (year 0) to 7% (year 62). Furthermore, an overall TC increase in these carbonate-containing agricultural soils will only occur: (i) during the initial rapid SOC sequestration accumulation phase (first 20 years of recultivation), and (ii) after the soils are fully decalcified (after ~62 years), but when SOC still slowly increases before SOC stocks reach full equilibrium (after ~197 years). However, compared with the initial TC stocks and considering periods of a semicentennial and beyond, we will likely lose more TC than we gain in these recultivated agricultural soils if there are no additional TC sequestration measures.

Funding

This work was supported by the National Science Foundation of China (No. 31370527, 30870414), Chinese Scholarship Council (scholarship No. 201706350210), German Federal Ministry of Education and Research (BMBF) in the INPLAMINT project (grant No. 031B0508A) and Towards a Sustainable Bioeconomy – Resources, Utilization, Engineering and AgroEcosystems (grant 2173).

Acknowledgements

We are grateful to individuals who helped with the field sampling and laboratory analysis during the 2 years of this study, especially Zhijie Li, Yunsheng Jia and Dr. Lutz Weihermüller (Forschungszentrum Jülich GmbH). Special thanks to the anonymous reviewers for their helpful comments that significantly improved the manuscript.

References:

Amelung, W., Bol, R., Friedrich, C., 1999. Natural C-13 abundance: a tool to trace the incorporation of dung-derived carbon into soil particle-size fractions. Rapid Commun. Mass Sp. 13: 1291-1294. https://doi.org/10.1002/(SICI)1097-0231(19990715)13:13<1291::AID-RCM637>3.0.CO;2-C

Amelung, W., Bossio, D., de-Vries, W., Kögel-Knabner, I., 2020. Towards a global-scale soil climate mitigation strategy. Nat. Commun. 1: 5427.

An, S., Huang, Y., Zheng, F., 2009. Evaluation of soil microbial indices along a revegetation chronosequence in grassland soils on the Loess Plateau, Northwest China. Appl. Soil Ecol. 41: 286-292. https://doi.org/10.1016/j.apsoil.2008.12.001

Batjes, N.H., 1996. Total carbon and nitrogen in the soils of the world. Eur. J. Soil Sci. 47: 151-163. https://doi.org/10.1111/j.1365-2389.1996.tb01386.x

Bol, R., Poirier, N., Balesdent, J., Gleixner, G., 2009. Molecular turnover time of soil organic matter in particle ‐ size fractions of an arable soil. Rapid Commun. Mass Sp. 23: 2551-2558. https://doi.org/10.1002/rcm.4124

Bughio, M.A., Wang, P.L., Meng, F.Q., Chen, Q., Yakov, K., Wang, X.J., Junejo, S.A., 2015. Neoformation of pedogenic carbonates by irrigation and fertilization and their contribution to carbon sequestration in soil. Geoderma 262: 12-19. https://doi.org/10.1016/j.geoderma.2015.08.003

Bughio, M.A., Wang, P.L., Meng, F.Q., Chen, Q., Li, J., Shaikh, T.A., 2017. Neoformation of pedogenic carbonate and conservation of lithogenic carbonate by farming practices and their contribution to carbon sequestration in soil. J. Plant Nutr. Soil Sc. 180: 454-463. https://doi.org/10.1002/jpln.201500650

Chevallier, T., Cournac, L., Hamdi, S., Gallali, T., Bernoux, M., 2016. Temperature dependence of CO_2 emissions rates and isotopic signature from a calcareous soil. J. Arid Environ. 135: 132-139. https://doi.org/10.1016/j.jaridenv.2016.08.002

Clayton, J., Lemanski, K., Bonkowski, M., 2021. Shifts in soil microbial stoichiometry and metabolic quotient provide evidence for a critical tipping point at 1% soil organic carbon in an agricultural post-mining chronosequence. Biol. Fert. Soils 57: 435-446. https://doi.org/10.1007/s00374-020-01532-2

Clean Energy Wire. 2018. Germany's three lignite mining regions. https://www.cleanenergywire.org/factsheets/germanys-three-lignite-mining-regions (last accessed 5 December 2021).

Coleman, K., Jenkinson, D.S., 2005. RothC-26.3. A model for turnover of carbon in soil, model description and windows users guide, IACR-Rothamsted, Harpenden.

544 Corwin, D.L., Lesch, S.M., 2003. Application of soil electrical conductivity to precision agriculture: theory,
545 principles, and guidelines. Agron. J. 95: 455-471. https://doi.org/10.2134/agronj2003.4550
546 Costantini, E.A.C., Antichi, D., Almagro, M., Hedlund, K., Sarno, G., Virto, I., 2020. Local adaptation strategies
547 to increase or maintain soil organic carbon operational groups within the European innovation partnership.
548 J. Rural Stud. 79: 102-115. https://doi.org/10.1016/j.jrurstud.2020.08.005
549 Derrien, D., Marol, C., Balabane, M., Balesdent, J., 2006. The turnover of carbohydrate carbon in a cultivated
550 soil estimated by ^{13}C natural abundances. Eur. J. Soil Sci. 57: 547-557. https://doi.org/10.1111/j.1365-
551 2389.2006.00811.x
552 DIN, 2017. German Institute for Standardisation (Deutsches Institut für Normung). Determination of total organic
553 carbon (TOC) by dry combustion (DIN EN 15936: 2012-11). Determination of total nitrogen using dry
554 combustion method (DIN EN 16168:2012-11). Beuth Verlag, Germany.
555 Entry, J.A., Sojka, R.E., Shewmaker, G.E., 2004. Irrigation increases inorganic carbon in agricultural soils.
556 Environ. Manage. 33: 309-317. https://doi.org/10.1007/s00267-003-9140-3
557 Falloon, P., Smith, P., Coleman, K., Marshall, S., 1998. Estimating the size of the inert organic matter pool from
558 total soil organic carbon content for use in the Rothamsted carbon model. Soil Biol. Biochem. 30: 1207-
559 1211. https://doi.org/10.1016/S0038-0717(97)00256-3
560 Firestone, M.K., Davidson, E.A., 1989. Microbiological Basis of NO and N_2O Production and Consumption in
561 Soil. In: M.O. Andreae and D.S. Schimel (M.O. Andreae and D.S. Schimel) (M.O. Andreae and D.S.
562 Schimels), John Wiley and Sons, Chichester, UK, pp. 7-21.
563 Grandy, A.S., Neff, J.C., 2008. Molecular C dynamics downstream: The biochemical decomposition sequence
564 and its impact on soil organic matter structure and function. Sci. Total Environ. 404: 297-307.
565 https://doi.org/10.1016/j.scitotenv.2007.11.013
566 Herbst, M., Welp, G., Macdonald, A., Jate, M., Hädicke, A., Scherer, H., Gaiser, T., Herrmann, F., Amelung,
567 W., Vanderborght, J., 2018. Correspondence of measured soil carbon fractions and RothC pools for
568 equilibrium and non-equilibrium states. Geoderma, 314: 37-46.
569 https://doi.org/10.1016/j.geoderma.2017.10.047
570 Huang, P., Zhang, J.B., Xin, X.L., Zhu, A.N., Zhang, C.Z., Ma, D.H., Zhu, Q.G., Yang, S., Wu, S.J., 2015.
571 Proton accumulation accelerated by heavy chemical nitrogen fertilization and its long-term impact on
572 acidifying rate in a typical arable soil in the Huang-Huai-Hai Plain. J. Integr. Agr. 14: 148-157.
573 https://doi.org/10.1016/S2095-3119(14)60750-4
574 IPCC, 2018. Global warming of 1.5°C. Intergovernmental Panel on Climate Change. https://www.ipcc.ch/sr15/
575 (last accessed 5 December 2021).
576 ISO 11277, 2020. Soil quality - Determination of particle size distribution in mineral soil material - Method by
577 sieving and sedimentation. https://www.beuth.de/en/standard/iso-11277/324323392 (last accessed 18 April
578 2022).
579 Kim, S., Zang, H., Mortimer, P., Shi, L.L., Li, Y.J., Xu, J.C., Ostermann, A., 2018. Tree species and recovery
580 time drives soil restoration after mining: a chronosequence study. Land Degrad. Dev. 29: 1738-1747.
581 https://doi.org/10.1002/ldr.2951
582 Lal, R., 2002. Carbon sequestration in dryland ecosystems of West Asia and North Africa. Land Degrad. Dev. 13:
583 45-59. https://doi.org/10.1002/ldr.477
584 Lal, R., 2007. Carbon management in agricultural soils. Mitig. Adapt. Strat. Gl. 12: 303-322.
585 https://doi.org/10.1007%2Fs11027-006-9036-7
586 Lal, R., 2008. Soil carbon stocks under present and future climate with specific reference to European
587 ecoregions. Nutr. Cycl. Agroecosys. 81: 113-127. https://doi.org/10.1007%2Fs10705-007-9147-x
588 Lal, R., 2009. Sequestering carbon in soils of arid ecosystems. Land Degrad. Dev. 20: 441-454.

https://doi.org/10.1002/ldr.934
Lal, R., 2013. Intensive agriculture and the soil carbon pool. J. Crop Improv. 27: 735-751. https://doi.org/10.1080/15427528.2013.845053
Lardner, T., George, S., Tibbett, M., 2015. Interacting controls on innate sources of CO_2 efflux from a calcareous arid zone soil under experimental acidification and wetting. J. Arid Environ. 122: 117-123. https://doi.org/10.1016/j.jaridenv.2015.07.001
Lehtinen, T., Schlatter, N., Baumgarten, A., Bechini, L., Krüger, J., Grignani, C., Zavattaro, L., Costamagna, C., Spiegel, H., 2014. Effect of crop residue incorporation on soil organic carbon and greenhouse gas emissions in European agricultural soils. Soil Use Manage. 30: 524-538. https://doi.org/10.1111/sum.12151
Lewis, D.E., White, J.R., Wafula, D., Athar, R., Dickerson, T., Williams, H.N., Chauhan, A., 2010. Soil functional diversity analysis of a bauxite-mined restoration chronosequence. Microb. Ecol. 59: 710-723. https://doi.org/10.1007%2Fs00248-009-9621-x
Li, C., Shi, L.L., Ostermann, A., Xu, J.C., Li, Y.J., Mortimer, P.E., 2015. Indigenous trees restore soil microbial biomass at faster rates than exotic species. Plant Soil 396: 151-161. https://doi.org/10.1007/s11104-015-2570-x
Li X.S., Sajjad R., Liu Z.J., Chen, Z.J., Zhou, J.B., 2017. Effects of application of nitrogen fertilizer and nitrification inhibitor on carbon dioxide emissions from calcareous soil (in Chinese). J. Agr. Environ. Sci. 36: 1658-1663.
Löw, P., Osterburg, B., Klages, S., 2021. Comparison of regulatory approaches for determining application limits for nitrogen fertilizer use in Germany. Environ. Res. Lett. 16: 055009 https://doi.org/10.1088/1748-9326/abf3de
Luo, Z.K., Wang, E., Sun, J.X.O., 2010. Soil carbon change and its responses to agricultural practices in Australian agro-ecosystems: a review and synthesis. Geoderma 155: 211-223. https://doi.org/10.1016/j.geoderma.2009.12.012
Meng, F.Q., Lal, R., Kuang, X., Ding, G., Wu, W.L., 2014. Soil organic carbon dynamics within density and particle-size fractions of aquic cambisols under different land use in northern China. Geoderma Reg. 1: 1-9. https://doi.org/10.1016/j.geodrs.2014.05.001
Minasny, B., Malone, B.P., Mcbratney, A.B., Angers, D.A., 2017. Soil carbon 4 per mille. Geoderma 292: 59-86. https://doi.org/10.1016/j.geoderma.2017.01.002
Monger, H.C., Kraimer, R.A., Khresat, S., Cole, D.R., Wang, X., Wang, J., 2015. Sequestration of inorganic carbon in soil and groundwater. Geology, 43: 375-378. http://dx.doi.org/10.1130/G36449.1
Mörchen, R., Lehndorff, E., Diaz, F.A., Moradi, G., Bol, R., Fuentes, B., Klumpp, E., Amelung, W., 2019. Carbon accrual in the Atacama Desert. Global Planet. Change 181: 102993. https://doi.org/10.1016/j.gloplacha.2019.102993
Nelder, J.A., Mead, R.A., 1965. A simplex method for function minimization. Comput. J. 7: 308-313. https://doi.org/10.1093/comjnl/7.4.308
Pan, G.X., 1999. Pedogenic carbonates in aridic soil of China and the significance in terrestrial carbon transfer (in Chinese). J. Nanjing Agr. University 22: 51-57.
Potter, P., Ramankutty, N., Bennett, E.M., Donner, S.D., 2010. Characterizing the spatial patterns of global fertilizer application and manure production. Earth Interact. 14: 1-22. https://doi.org/10.1175/2009EI288.1
Raza, S., Miao, N., Wang, P.Z., Ju, X.T., Chen, Z.J., Zhou, J.B., Kuzyakov, Y., 2020. Dramatic loss of inorganic carbon by nitrogen-induced soil acidification in Chinese croplands. Global Change Biol. 26: 3738-3751. https://doi.org/10.1111/gcb.15101
Reichel, R., Hansch, M., Brüggemann, N., 2017. Indication of rapid soil food web recovery by nematode-derived indices in restored agricultural soil after open-cast lignite mining. Soil Biol. Biochem. 115: 261-264.

https://doi.org/10.1016/j.soilbio.2017.08.020
Roy, J., Reichel, R., Bruggemann, N., Hempel, S., Rillig, M.C., 2017. Succession of arbuscular mycorrhizal fungi along a 52-year agricultural recultivation chronosequence. Fems Microbiol. Ecol. 93: https://doi.org/10.1093/femsec/fix102
Rumpel, C., Amiraslani, F., Koutika, L.S., Smith, P., Whitehead, D., Wollenberg, E., 2018. Put more carbon in soils to meet Paris climate pledges. Nature 564: 32-34. https://www.nature.com/articles/d41586-018-07587-4
Rumpel, C., Amiraslani, F., Chenu, C., Cardenas, M.G., Kaonga, M., Koutika, L.S., Ladha, J., Madari, B., Shirato, Y., Smith, P., Soudi, B., Soussana, J.F., Whitehead, D., Wollenberg, E., 2020. The 4p1000 initiative: opportunities, limitations and challenges for implementing soil organic carbon sequestration as a sustainable development strategy. Ambio 49: 350-360. https://doi.org/10.1007%2Fs13280-019-01165-2
Sahrawat, K.L., 2003. Importance of inorganic carbon in sequestering carbon in soils of the dry regions. Curr. Sci. 84: 864-865. http://oar.icrisat.org/id/eprint/3945
Schmid, C., Reichel, R., Schröder, P., Brüggemann, N., Schloter, M., 2020. 52 years of ecological restoration following a major disturbance by opencast lignite mining does not reassemble microbiome structures of the original arable soils. Sci. Total Environ. 745: 140955. https://doi.org/10.1016/j.scitotenv.2020.140955
Schwenke, G.D., Ayre, L., Mulligan, D.R., Bell, L.C., 2000. Soil stripping and replacement for the rehabilitation of bauxite-mined land at Weipa. II. Soil organic matter dynamics in mine soil chronosequences. Aust. J. Soil Res. 38: 371-393. https://doi.org/10.1071/SR99043
Six, J., Jastrow, J.D., 2002. Organic matter turnover, in Lal, R.: Encyclopedia of Soil Science. Marcel Dekker, Boca Raton, FL, USA, 936-942.
Six, J., Conant, R.T., Paul, E.A., Paustian, K., 2002. Stabilization mechanisms of soil organic matter: implications for C-saturation of soils. Plant Soil 241: 155-176. https://doi.org/10.1023/A:1016125726789
Soussana, J.F., Lutfalla, S., Ehrhardt, F., Rosenstock, T., Lamanna, C., Havlík, P., Richards, M., Wollenberg, E., Chotte, J.L., Torquebiau, E., Ciais, P., Smith, P., Lal, R., 2019. Matching policy and science: rationale for the '4 per 1000-soils for food security and climate' initiative. Soil Till. Res. 188: 3-15. https://doi.org/10.1016/j.still.2017.12.002
Spiertz, J.H.J., Ewert, F., 2009. Crop production and resource use to meet the growing demand for food, feed and fuelopportunities and constraints. NJAS-Wagen. J. Life Sc. 56: 281-300. https://doi.org/10.1016/S1573-5214(09)80001-8
Stahl, P.D., Jonathan, D.A., Lachlan, J.I., Gerald, E.S., Daniel, L.M., 2003. Accumulation of oganic carbon in reclaimed coal mine soils of wyoming, National Meeting of the American Society of Mining and Reclamation and The 9th Billings Land Reclamation Symposium, pp. https://doi.org/10.21000/JASMR03011206
Stockmann, U., Adams, M.A., Crawford, J.W., Field, D.J., Henakaarchchi, N., Zimmermann, M., 2013. The knowns, known unknowns and unknowns of sequestration of soil organic carbon. Agr. Ecosyst. Environ. 164: 80-99. https://doi.org/10.1016/j.agee.2012.10.001
Tamir, G., Shenker, M., Heller, H., Bloom, P.R., Fine, P., Bar-Tal, A., 2013. Organic N mineralization and transformations in soils treated with animal waste in relation to carbonate dissolution and precipitation. Geoderma 209-210: 50-56. https://doi.org/10.1016/j.geoderma.2013.05.028
Vindušková, O., Frouz, J., 2013. Soil carbon accumulation after open-cast coal and oil shale mining in Northern Hemisphere: a quantitative review. Environ. Earth Sci. 69: 1685-1698. https://doi.org/10.1007/s12665-012-2004-5
Von Lützow, M., Kögel-Knabner, I., Ekschmitt, K., Flessa, H., Guggenberger, G., Matzner, E., Marschner, B., 2007. SOM fractionation methods: Relevance to functional pools and to stabilization mechanisms. Soil

Biol. Biochem. 39: 2183-2207. https://doi.org/10.1016/j.soilbio.2007.03.007
Weihermüller, L., Graf, A., Herbst, M., Vereeecken, H., 2013. Simple pedotransfer functions to initialize reactive carbon pools of the RothC model. Eur. J. Soil Sci. 64: 567-575. https://doi.org/10.1111/ejss.12036
Wendt, J.W., Hauser, S., 2013. An equivalent soil mass procedure for monitoring soil organic carbon in multiple soil layers. Eur. J. Soil Sci. 64:58-65. https://doi.org/10.1111/ejss.12002
Yu, W.J., Li, X.S., Chen, Z.J., Zhou, J.B., 2018. Effects of application of nitrogen fertilizer on carbon dioxide emissions from soils with different inorganic carbon contents (in Chinese). Chinese J. Appl. Ecology, 29: 2493-2500.
Zamanian, K., Kuzyakov, Y., 2018. Contribution of soil inorganic carbon to atmospheric CO_2: more important than previously thought. Global Change Biol. 25: e1-e3. https://doi.org/10.1111/gcb.14463
Zamanian, K., Zarebanadkouki, M., Kuzyakov, Y. (2018). Nitrogen fertilization raises CO_2 efflux from inorganic carbon: A global assessment. Global Change Biol. 24: 2810-2817. https://doi.org/10.1111/gcb.14148
Zhang, Y., Mu, Y., Zhou, Y., Tian, D., Liu, J.F., Zhang, C.L., 2016. NO and N_2O emissions from agricultural fields in the North China Plain: origination and mitigation. Sci. Total Environ. 551-552: 197-204. https://doi.org/10.1016/j.scitotenv.2016.01.209
Zhao, Y., Wu, S.X., Bol, R., Bughio, M.A., Wu, W.L., Hu, Y.C., Meng, F.Q., 2020. Intensive organic vegetable production increases soil organic carbon but with a lower carbon conversion efficiency than integrated management. J. Plant Nutr. Soil Sc. 183: 155-168. https://doi.org/10.1002/jpln.201900308
Zhao, Y., Bol, R., Sun, Z.A., Zhu-ge, Y.P., Shi, X.X., Wu, W.L., Meng, F.Q., 2021. CO_2 emission and source partitioning from carbonate and non-carbonate soils during Incubation. Pedosphere http://pedosphere.issas.ac.cn/trqcn/ch/reader/create_pdf.aspx?file_no=pedos202001011
Zheng, Y., Cao, X., Jiang, L., 2019. Problems and measures of ecological environment restoration for open-pit mining area (in Chinese). Shanxi Forest Sci. Technol. 47: 92-94.
Zhu, J.Y., Lücke, A., Wissel, H., Müller, D., Mayr, C., Ohlendorf, C., Zolitschka, B., 2013. The last glacialeInterglacial transition in patagonia, argentina: the stable isotope record of bulk sedimentary organic matter from Laguna Potrok Aike. Quaternary Sci. Rev. 71: 205-218. https://doi.org/10.1016/j.quascirev.2012.05.025
Zopes, E.M.G., 2017. Development of the humus reserves of recultivated agricultural areas of different ages in the Rhenish lignite district (in German), University of Bonn, Bonn.

Figure Click here to access/download;Figure;Figure 4.20.docx

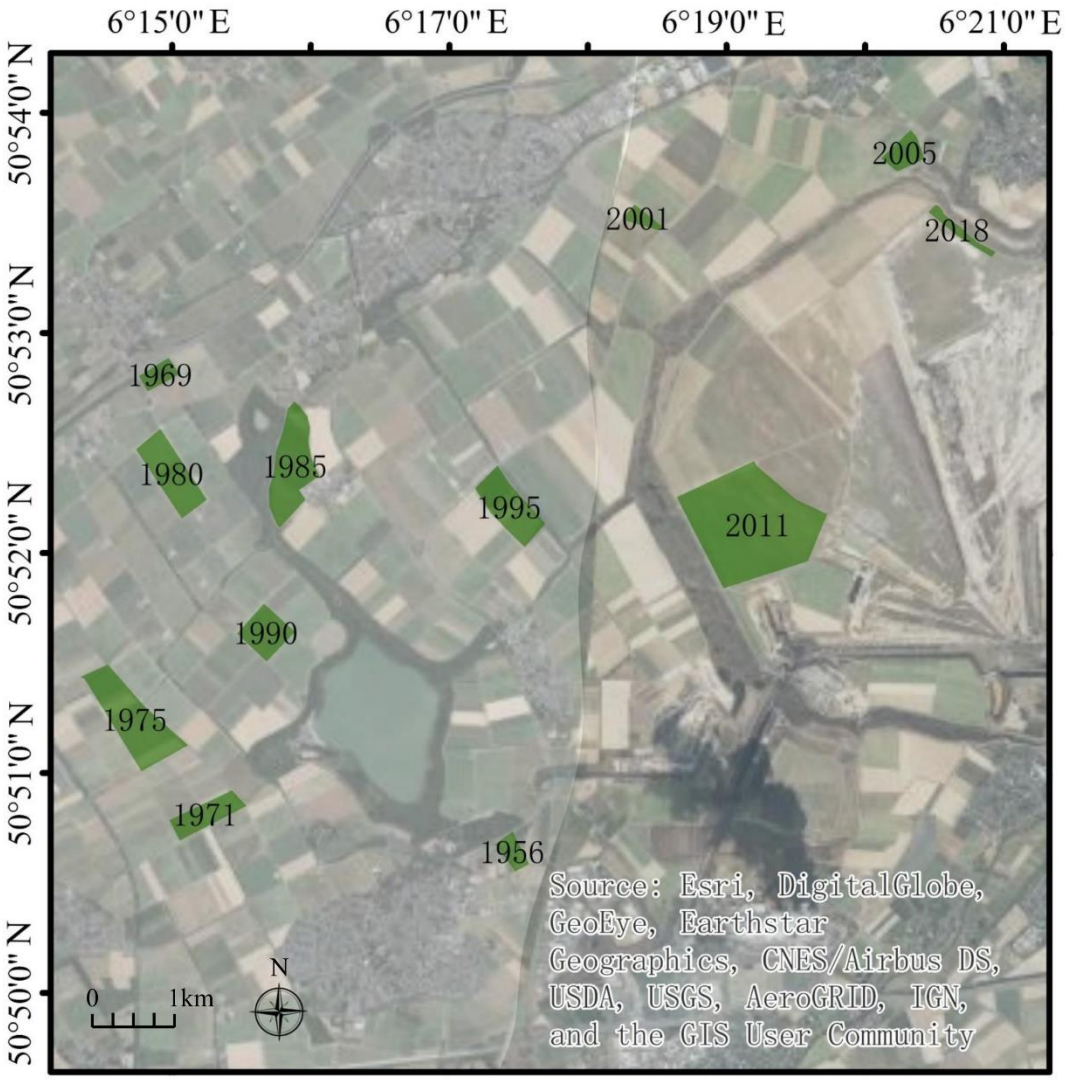

Fig 1. Location map of fields and year of recultivation.

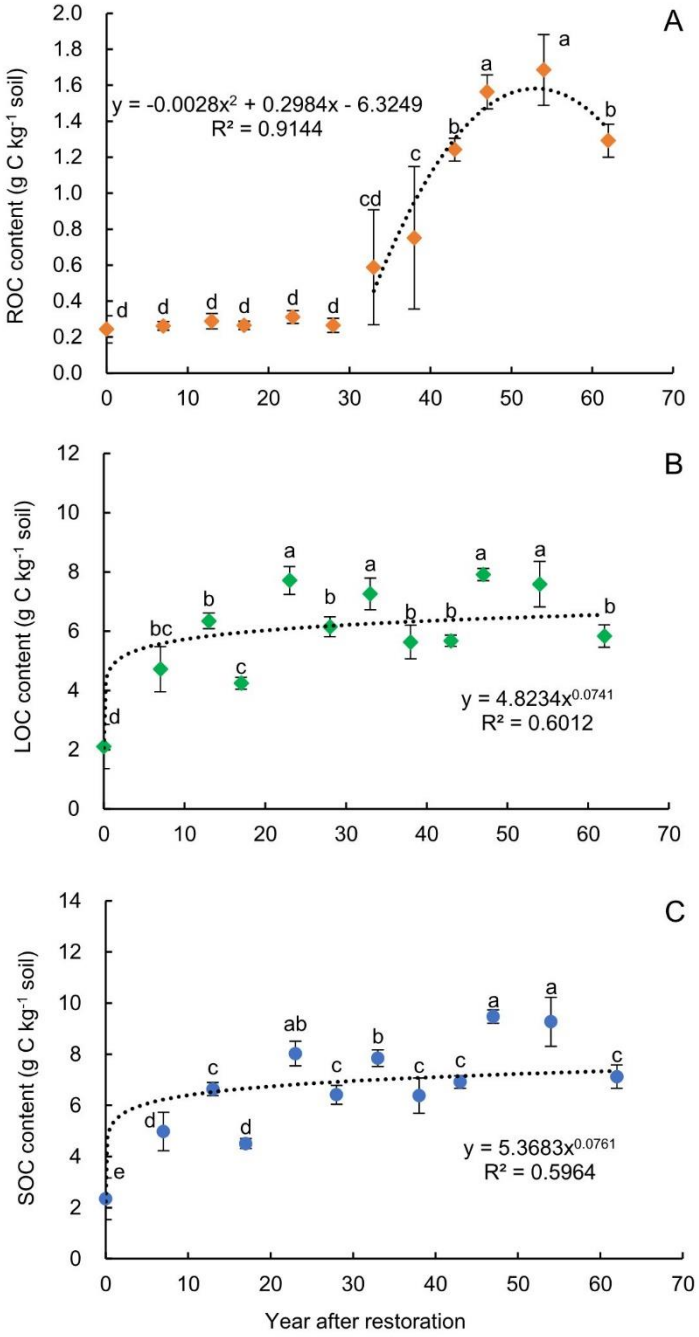

Fig. 2 ROC and SOC contents along 62-year agricultural recultivation chronosequence.

Note: Bars show standard deviation (n=5). Different lower-case letters indicate there have significant differences between the restored farmland (P<0.05).

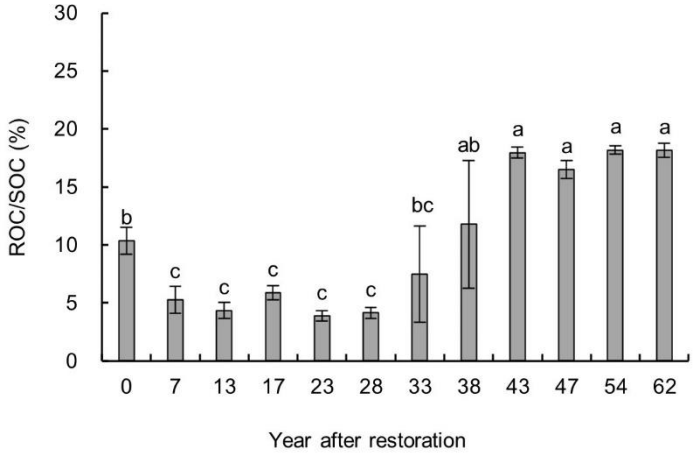

Fig. 3 ROC/ SOC along 62-year agricultural recultivation chronosequence.

Note: Bars show standard deviation (n=5). Different lower-case letters indicate there have significant differences between the restored farmland (P<0.05).

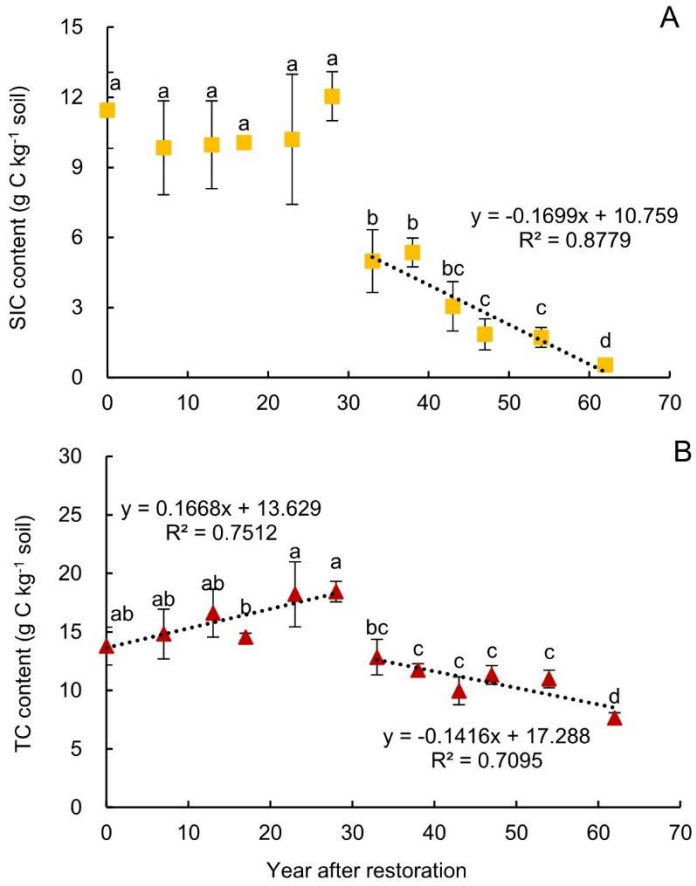

Fig. 4 SIC and TC contents along 62-year agricultural recultivation chronosequence.

Note: Bars show standard deviation (n=5). Different lower-case letters indicate there have significant differences between the restored farmland (P<0.05).

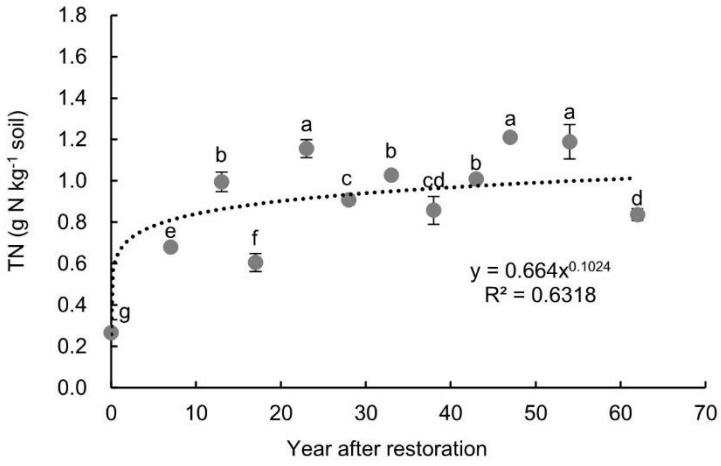

Fig. 5 TN contents along 62-year agricultural recultivation chronosequence.

Note: Bars show standard deviation (n=5). Different lower-case letters indicate there have significant differences between the restored farmland (P<0.05).

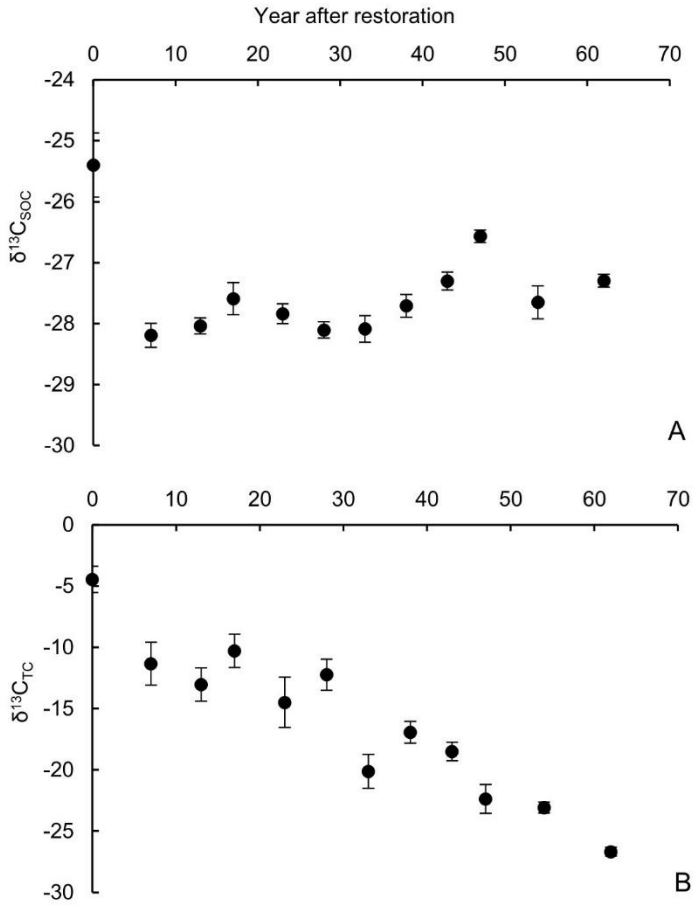

Fig. 6 $\delta^{13}C_{SOC}$ and $\delta^{13}C_{TC}$ contents along 62-year agricultural recultivation chronosequence.

Note: Bars show standard deviation (*n*=5).

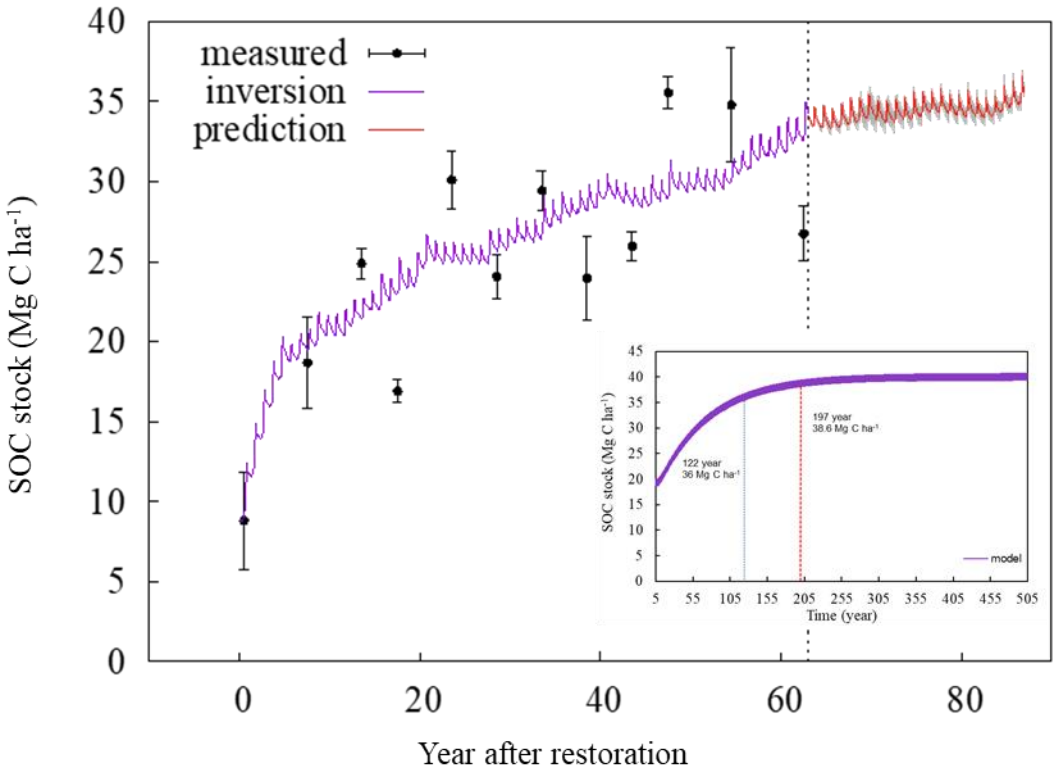

Fig. 7 Evolution of measured and simulated SOC stocks.

Note: The grey surface represents the standard deviation of SOC prediction according to 100 realisations of temperature data. Bars show standard deviation (n=5). The figure inserted in the lower right corner indicates: Roth C model predicts the SOC stock equilibrium of restored farmland. The equilibrium state was reached after 197 years, linked with an equilibrium SOC stock of 38.6 Mg C ha^{-1}; A level of 36 Mg C ha^{-1}, being reasonably close to the equilibrium SOC stock, was already met after 122 years.

Table Click here to access/download;Table;Table 4.20.docx

Table 1 Initial SOC (Mg ha^{-1}) and pools and estimated SOC (Mg ha^{-1}) and pools for December 2018.

	Soil organic carbon (SOC)	Decomposable plant material (DPM)	Resistant plant material (RPM)	Microbial biomass (BIO)	Humified organic matter (HUM)
year 0	8.80	0	1.22	0.15	6.85
62 years later	34.17	0.46	8.26	0.96	23.90

Table 2 Soil foundation properties along 62-year agricultural recultivation chronosequence.

year	pH	Electrical conductivity （uS/cm）	Bulk density （g cm^{-3}）	Sand (%)	Silt （%）	Clay （%）
0	7.2±0.02a	62.8±3.5cde	1.17±0.11c	4.9±1.0cde	78.6±1.3bcde	16.5±1.8cd
7	7.3±0.08a	68.6±4.5cde	1.25±0.04b	8.1±0.3a	76.1±0.9fgh	15.8±0.9d
13	7.1±0.03b	85.4±18.2bcd	1.29±0.06ab	6.4±1.3abc	77.4±1.4cdef	16.3±0.4d
17	7.0±0.05b	56.2±9.4e	1.32±0.08ab	3.0±0.9f	79.3±0.9abc	17.7±0.5abc
23	7.0±0.04bc	100.9±13.3ab	1.29±0.08ab	4.8±0.2cdef	79.0±0.2bcde	16.2±0.3d
28	7.0±0.05bc	120.2±18.8ab	1.31±0.07ab	3.2±0.3ef	81.2±1.7a	15.5±1.0d
33	6.9±0.04cd	63.8±4.3cde	1.32±0.05ab	3.7±0.3def	79.4±0.6ab	16.9±0.2bcd
38	6.9±0.07cd	80.3±17.4abc	1.24±0.01bc	5.5±0.7bcd	76.7±1.1efg	17.8±1.3abc
43	6.9±0.07cd	163.7±48.9a	1.36±0.06a	5.4±0.5cd	75.9±0.6fgh	18.6±0.3a
47	6.8±0.04d	56.6±6.1e	1.31±0.08ab	4.1±1.3def	77.2±1.1def	18.7±0.7a
54	6.9±0.04cd	47.6±14.2cde	1.26±0.02ab	7.3±0.5ab	74.6±0.5dh	18.0±0.4ab
62	6.4±0.19d	47.4±12.1ce	1.25±0.01b	6.6±2.8abc	74.9±2.4f	18.5±0.5a

Note: Data are mean±SD (n=5). Different lowercase letters indicate LSD (P<0.05) significant difference between agricultural recultivation chronosequence.

Table 3 Soil carbon stock along 62-year agricultural recultivation chronosequence.

(year)	SOC (Mg C ha^{-1})	SIC (Mg C ha^{-1})	TC (Mg C ha^{-1})
0	8.2±2.9g	40.0±1.7b	48.2±5.7e
7	18.7±2.8f	37.0±7.6b	55.7±8.0d
13	25.7±1.0de	38.7±7.3b	64.4±8.0bc
17	17.8±0.8f	39.7±1.0b	57.5±1.3cd
23	31.0±1.9b	39.4±5.8b	70.4±10.7ab
28	25.1±1.4de	47.2±2.1a	72.3±3.4a
33	31.0±1.3b	19.7±5.3c	50.7±6.0de
38	23.8±2.6e	19.9±2.3c	43.7±2.1ef
43	28.3±1.0c	12.5±4.3d	40.8±4.9f
47	37.1±1.0a	7.3±2.6de	44.4±3.1ef
54	35.1±3.6a	6.5±1.6de	41.6±2.9f
62	26.7±1.7cd	2.0±0.5e	28.7±1.7e

Note: Data are mean±SD (n=5). Different lower-case letters mean LSD (P<0.05) significant difference between the restored farmland.

Declaration of interests

☒The authors declare that they have no known competing financial interests or personal relationships that could have appeared to influence the work reported in this paper.

☐The authors declare the following financial interests/personal relationships which may be considered as potential competing interests:

Click here to access/download
Supplementary Material
Supplemenral File 7.9.docx